

Nowcast Guidance of Afternoon Convection Initiation Using TANC

Hui-Ling Chang¹, Barbara G. Brown³, Pao-Shin Chu⁴, Yu-Chieng Liou⁵, and Wen-Ho Wang²

1. Research and Development Center, Central Weather Bureau, Taipei, Taiwan

2. Meteorological Satellite Center, Central Weather Bureau, Taipei, Taiwan

3. National Center for Atmospheric Research, Boulder, Colorado, USA

4. Department of Atmospheric Sciences, School of Ocean and Earth Science and Technology, University of Hawaii, Honolulu, Hawaii

5. Department of Atmospheric Sciences, National Central University, Jhong-Li, Taiwan

Abstract

Focusing on afternoon thunderstorms in Taiwan during the warm season (May- October) under weak synoptic forcing, this study applied the Taiwan Auto-NowCaster (TANC) to produce 1-h likelihood nowcasts of afternoon convection initiation (ACI) using a fuzzy logic approach. The primary objective is to design more useful forecast products with uncertainty regions of predicted thunderstorms to provide nowcast guidance of ACI for forecasters.

Three sensitivity tests on forecast performance were conducted to improve the usefulness of nowcasts for forecasters. The optimal likelihood threshold (L_t) for ACIs, which is the likelihood value that best corresponds to the observed ACIs, was determined to be 0.6. Because of the high uncertainty on the exact location or timing of ACIs in nowcasts, location displacement and temporal shifting of ACIs should be considered in operational applications. When a spatial window of 5 km and a temporal window of 18 min are applied, the TANC displays moderate accuracy and satisfactory discrimination with an acceptable degree of over-forecasting.

Keywords: afternoon convection initiation (ACI), fuzzy logic approach, likelihood nowcasts, uncertainty

1. Introduction

For short-range (0–6 hr) forecasts, one of the most challenging tasks is to predict whether a convective storm will occur, as well as when and where it will happen. Relative to other convective systems, such as stationary fronts and typhoons, forecasting afternoon convective storms is more difficult because of their small spatial scale and very short lifetime.

Rapidly intensifying afternoon convections can lead to lightning strikes and heavy downpours, which may cause problems such as power failures, traffic jams, flooding, and aviation hazards. Accurate nowcasts gain disaster management agencies valuable additional lead-time to implement appropriate preventive actions against severe weather. Improving nowcasts of afternoon thunderstorms is one of the research priorities of the Central Weather Bureau (CWB) in Taiwan.

Currently, nowcasts of afternoon convective storms using numerical models are challenging. One reason for this is the crude representations of model physics and convective schemes (Roberts et al. 2012). Another reason is that crucial characteristics of mesoscale boundaries, such as the frontal edges of land or sea breezes and

anabatic or katabatic winds, cannot be adequately resolved by operationally available radar observations (when the boundaries are too far away from the radar, or too shallow for the radar to detect) or surface observations (generally sparsely spaced) used to initialize model fields in Taiwan. Therefore, mesoscale boundary information is unavailable in model initial fields. However, such information is critical for producing accurate forecasts of afternoon convection initiations (ACIs) using dynamical models. One way to mitigate this problem is to apply a statistical forecasting technique such as a fuzzy logic algorithm to mesoscale predictors that can be observed or forecast.

Focusing on ACIs in Taiwan under weak synoptic forcing, we applied the Taiwan Auto-NowCaster (TANC) to produce 1-h likelihood nowcasts of CI based on a fuzzy logic approach. Eight predictors were used in the study, and two of them were based on the radar climatology constructed by Lin et al. (2012). In this study we evaluate the forecast performance of the TANC in order to establish a reference for its future development and improvement. The ultimate goal is to provide forecasters with more useful nowcast products for guidance on ACIs in Taiwan.

This paper is organized as follows. The TANC and study data are introduced in Section 2. The verification and analysis methodology are presented in Section 3. Section 4 describes the sensitivity experiments on verification scores, including the sensitivity of scores to likelihood thresholds, spatial windows, as well as different combination of spatial and temporal windows. A summary of the findings and suggestions for future research are provided in Section 5.

2. TANC and study data

The TANC was introduced to the CWB by the U.S. National Center for Atmospheric Research (NCAR) and was created specifically to predict convective storms on a subtropical island with high mountains and complex terrain. The TANC covers Taiwan and its adjacent seas with a 0.01° horizontal resolution; the system estimates the 1-h likelihood of CI every 6 min operationally. CI is defined as new convection with reflectivity ≥ 35 dBZ.

The TANC nowcasts the likelihood of CI using eight predictors based on a fuzzy logic approach. Specifically, the predictor values are converted into likelihood values through fuzzy membership functions, which are derived from the statistics of pre-storm environmental characteristics, climatology of radar reflectivity, and so on. “Fuzzy” indicates that the likelihood values range from -1 to 1 . Higher positive values indicate an increased likelihood of CI in a region, lower negative values indicate a decreased likelihood, and 0 indicates a neutral likelihood (Mueller et al. 2003).

The conceptual models of TANC are based on determining the overlap of regions with a high climatological frequency and trend of convective storms, high instability, surface convergence, and other favorable conditions for triggering convection. The overlap regions of the various predictors are also the expected regions of CI (Mueller et al. 2003).

This study focuses on well-organized afternoon convective storms under weak synoptic forcing in May–October. Nine days of afternoon convective storms that occurred in Taiwan from 2014 to 2015 were chosen for evaluation and a total of 312 1-h nowcasts were verified.

3. Verification methodology

a. Conversion from likelihood to Y/N forecasts

The TANC provides 1-h likelihood nowcasts of ACI, which indicate the uncertainty information associated with forecasts. Note that a likelihood nowcast is different from a probabilistic forecast, even if both have a similar

meaning—higher value represents higher possibility. The likelihood values from the TANC range from -1 to 1 while the probability is bounded between 0 and 1 . Because the TANC likelihood nowcast is not probabilistic forecast, forecasters need to know how to best use the TANC nowcasts. Another problem is that the TANC frequently shows large areas of low likelihood values (< 0.3) for CI, which results in forecasters mistakenly believing that CI may occur everywhere. To provide guidance on the most likely region for CI, we attempt to determine an optimal likelihood threshold (L_t) that best corresponds to the observed CI. Therefore, the likelihood forecasts are converted into Y/N forecasts. Moreover, the forecast uncertainty information is incorporated in the final nowcast products using the relaxation method described later. The conversion from likelihood to Y/N forecasts is performed by first selecting a relevant L_t . For example, if the L_t is 0.8 then if the likelihood exceeds this threshold it means that the TANC predicts there is new convection in the next hour. Otherwise, the prediction is classified as a nonevent.

Currently, there is no direct observation that can unambiguously indicate whether new convection has initiated within the past hour. However, we need such information to determine whether the TANC nowcasts are correct. Here we adopt the same approach as Lakshmanan et al. (2012). Two radar images 1-hr apart were examined to find where new convection has occurred. The past observation was warped to best align it with the current observation using a cross-correlation optical flow method. This involves finding a smooth motion field based on the two images and then advecting the corresponding grid in the second image backward to align it with the first one. Once the two images have been aligned, a 5×5 neighborhood (~ 5 km) of each pixel was searched to determine the convective state within the past hour. Each pixel of the radar image was then classified into one of four categories: new; ongoing; decaying; and no convection.

By using the aforementioned conversion, each gridpoint was classified into one of four possible conditions in a 2×2 contingency table (Table 1), consequently enabling computation of the threat score (TS), bias ratio (BIAS), probability of detection (POD), false alarm ratio (FAR), Kuiper score (KS), and Equitable threat score (ETS) for the forecast verification.

b. Relaxation method

Compared with forecasting other weather systems,

the uncertainty for ACI nowcasts is considerably higher. All kinds of uncertainties during the forecast process result in difficulty in predicting the exact location and timing of ACIs. Therefore, the location displacement and temporal shift of predicted storms should be accounted for in operational applications. The primary purpose of this study is to describe an approach to represent the most likely regions for ACIs with uncertainty information on nowcast products, and provide more useful guidance on ACIs for forecasters. What should the space-time tolerances be to achieve a level of accuracy that is considered acceptable? This question is addressed through the development of a relaxation method using a historical ACI dataset, and taking into account the operational needs of forecasters in Taiwan.

1) Spatial relaxation

For location displacement, we relax restrictions from a pixel-to-pixel verification to a verification of a circle with a radius of N gridpoints. This spatial relaxation method is similar to Lakshmanan et al. (2012), but with a modification to render uniform location displacement in all directions. In Lakshmanan et al. (2012), the pixel-to-pixel verification was relaxed to a verification of a square area of $(2N+1)(2N+1)$ gridpoints (Fig. 1). As a result, the tolerable location displacement of a predicted storm is larger in the diagonal than the other radial directions. To overcome this issue, the area of tolerable location displacement was modified to a circle with radius of N gridpoints.

Figure 1 illustrates the spatial relaxation method with $N = 1$, which means only one gridpoint of location displacement is an acceptable tolerance for the CI nowcasts. Suppose that the TANC predicted a certain gridpoint as CI. If a pixel-to-pixel verification was applied, this gridpoint would be classified as a “hit (h)” only when new convection was observed at the same gridpoint in the verification field. However, if one gridpoint of location displacement was allowed ($N = 1$), this verifying gridpoint would be regarded as h when new convection was observed within a circle with radius of one gridpoint. Therefore, allowing for location displacement increases the frequency of h . A “false alarm (f)” requires the nowcast to predict CI but without new convection observed at the same gridpoint through a pixel-to-pixel verification; however, under the $N = 1$ relaxation, this gridpoint would be classified as f if no new convection was observed within a circle with radius of one gridpoint. Therefore, allowing for location

displacement reduces the frequency of f .

A “miss (m)” requires new convection to be observed but no CI to be predicted at the same gridpoint using a pixel-to-pixel verification; however, under the $N = 1$ relaxation, this gridpoint would be classified as m if no CI was predicted within a circle with radius of one gridpoint. Therefore, allowing for location displacement reduces the frequency of m . None of the aforementioned categories would be classified as a “correct rejection (c)” in the contingency table (Table 1). The spatial relaxation works favorably because the horizontal resolution of the TANC is high (~ 1 km). The smoothed forecasts will generally have better verification scores than the unsmoothed forecasts.

2) Temporal relaxation

Temporal relaxation is also accounted for in the verification of CI nowcasts. Suppose a temporal window ($T = 18$ min) is considered, which means a temporal shift of less than 18 min is an acceptable tolerance for the CI nowcasts. That is, if the TANC 1-h nowcast predicts CI, the new convection is expected to occur in the next 42 to 78 min ($1 \text{ h} \pm 18 \text{ min}$). If the initial time of the 1-h CI nowcast was 0630 UTC, the predicted new convection would likely occur between 0712 and 0748 UTC ($0730 \text{ UTC} \pm 18 \text{ min}$) under the $T = 18$ min relaxation. In other words, the new convection predicted by the TANC nowcasts between 0612 and 0648 UTC ($0630 \text{ UTC} \pm 18 \text{ min}$) would probably occur at 0730 UTC (Fig. 2a; temporal window setting I).

However, timing of the temporal window also needs to take into account the operational needs of the forecasters to have the latest information at the time that they must produce their forecasts. Based on the viewpoint of operational applications, only the forecasts that have already been generated (i.e., the forecasts issued earlier than 0630 UTC) can be used to provide additional information for the latest 1-h nowcast (i.e., the forecast issued at 0630 UTC). Therefore, we tested whether the forecast performance will be severely affected if the nowcast is set at the ending point of the temporal window (Fig. 2b; temporal window setting II) given the same window size.

The result indicates that the forecast performance of TANC is more sensitive to the window length than to the ending point of the temporal window. The forecast performance will not be severely affected if the nowcast is set at the ending point of the temporal window, given the same window size. Therefore, for operational

considerations, we adopt the window setting II to determine the most adequate temporal shift of predicted storms. The temporal relaxation works well because the temporal resolution of the TANC is high (6 min).

In Section 4, which focuses on sensitivity experiments, we apply the spatial and temporal relaxation method to evaluate the forecast performance of the TANC under different spatial and temporal windows. Based on the evaluation results, we determine the most likely regions and the less likely, but still possible, areas for CI for TANC nowcast products.

4. Sensitivity experiments

In this section, sensitivity tests for various L_t were conducted to determine an optimal L_t to provide guidance on the most likely region for CI. In addition, sensitivities of verification scores to different spatial ($\pm 1-10$ km) and temporal (6–36 min) windows were also investigated to determine acceptable spatial and temporal uncertainty ranges for the purpose of displaying the less likely, but still possible, regions for CI.

a. Sensitivity of scores to different L_t s

The forecast performance for no relaxation at different L_t s (Fig. 3) shows that the median TS and FAR values do not greatly vary when L_t is between 0.3 and 0.6; however, the median BIAS and POD values exhibit a clear decrease with increasing L_t . The optimal L_t is selected using the following arguments: A lower L_t produces a higher POD, but also leads to over-forecasting. Therefore, the POD alone should not be used for determining the optimal L_t . With a focus on the BIAS, the ratio is too large when L_t is between 0.3 and 0.5. When L_t equals 0.6, the TANC displays an acceptable degree of over-forecasting. If L_t is increased to 0.7, the TANC exhibits under-forecasting ($\text{BIAS} < 1$), and the TS decreases considerably. Thus, an L_t of 0.6 is selected as the optimal value for 1-h nowcasts of ACIs.

b. Sensitivity of scores to different spatial windows

Figure 4 displays the score median with a 95% confidence interval associated with different spatial windows when the optimal L_t (0.6) was applied. When the spatial window (N) equals zero, the verification results were determined using a pixel-to-pixel verification. When N was extended out to five gridpoints, the median TS, BIAS, KS, and ETS values were approximately 0.33, 1.87, 0.84, and 0.33, respectively. In this case the TANC displayed moderate accuracy and satisfactory

discrimination but also an acceptable degree of over-forecasting. The values of the ETS and TS are similar because ACIs can be regarded as rare events in the TANC domain and the chance of random hits is very low for the TS. For this reason we only show the TS in the latter analysis. In addition, the KS approaches the POD for rare events; thus, we use the KS together with the BIAS to evaluate the forecast quality of TANC to ensure that the high value of KS does not result from serious overforecasting. The 95% confidence intervals were narrow, indicating that the uncertainty caused by sampling variability or limitations in sample size is very small.

Regarding the aforementioned two sensitivity tests, the CWB provides one formulation of the operational TANC nowcast product with an optimal L_t of 0.6 and a spatial window of five gridpoints (Fig. 5a). Figure 5b shows the same nowcast product using the spatial relaxation from Lakshmanan et al. (2012) for comparison. When adopting a square of $(2N+1)(2N+1)$ gridpoints as the area of tolerable location displacement, the boundary of the uncertainty area of ACI will have a zigzag or square shape. In other words, the tolerable location displacement is not identical in all directions. Therefore, we opt to use a circle with a radius of N gridpoints as the area of tolerable location displacement.

Five gridpoints were selected as the spatial window for the TANC for two reasons: (i) the KS becomes saturated with this setting (Fig. 4); and (ii) a location displacement of five gridpoints (~ 5 km) is the maximum tolerable range considered by forecasters due to the small size of Taiwan.

c. Sensitivity of scores to different combinations of spatial and temporal windows

The results of sensitivity tests when spatial and temporal windows are combined (Fig. 6) showed that both expanding spatial windows and lengthening temporal windows would yield better verification scores. Focusing on the KS, the saturation point is almost at the spatial window of five gridpoints and the temporal window of 18 min. Adopting this window setting as the forecast guidance of ACIs, the TS, BIAS, and KS values are 0.43, 1.81, and 0.94, respectively. That is, the TANC displayed moderate accuracy and satisfactory discrimination, but also an acceptable degree of over-forecasting. According to the results from the three aforementioned sensitivity tests, the CWB provides a TANC nowcast product for ACIs with an optimal L_t of

0.6, spatial window of five gridpoints, and temporal window of 18 mins (Fig. 6)

5. Conclusion and Ongoing Work

Focusing on nine days of afternoon thunderstorms under weak synoptic forcing in 2014 and 2015, we apply the TANC to generate 1-h likelihood nowcasts of ACIs based on a fuzzy logic approach. The primary purpose is to provide more useful nowcast guidance of ACIs for forecasters.

Sensitivity experiments for various Lts were conducted to determine the optimal Lt for indicating ACI. The criterion of threshold selection is to balance the hits against false alarms (or POD against BIAS) in the ACI forecasts. A higher POD, which indicates a greater chance of ACI being detected, is not necessarily the best choice. The optimal value of Lt for ACI is suggested to be 0.6. The sensitivity experiments on spatial and temporal windows showed that a combination of a spatial window of 5 km and a temporal window of 18 min is preferred as the acceptable uncertainty range of forecast errors when operational needs are taken into account. Under this condition, the TANC displays moderate accuracy and satisfactory discrimination with an acceptable degree of over-forecasting.

Based on the results from sensitivity experiments, we designed a new nowcast product that only displays the most likely regions (Fig. 7 in pink) for ACIs (i.e., the areas with $Lt \geq 0.6$) instead of likelihood contours. In addition, the tolerable areas of storm displacement (5 km) and temporal shift (18 min) are also shown to indicate the less likely, but still possible, areas of ACIs (Fig. 7 in blue).

To produce more accurate ACI nowcasts, some predictors of the TANC should be changed. Among the eight predictors, three predictors come from the analysis field of the regional CWB-WRF model, which is updated every six hours with a horizontal resolution of 15 km. Additionally, the surface divergence predictor is calculated from wind observations at stations with a spacing of approximately 9–10 km. The temporal and spatial resolutions of these four predictors are too low to resolve the atmospheric characteristics required for ACI nowcasts. At present, analysis fields of the STMAS-WRF model should be considered as replacements for their equivalents in the CWB-WRF model to provide higher temporal and spatial resolution information on wind, thermal, and humidity fields.

Reference

Lakshmanan, V., J. Crockett, K. Sperow, M. Ba, and L. Xin, 2012: Tuning AutoNowcaster automatically. *Wea. Forecasting*, **27**, 1568–1579.

Lin, P. F., P. L. Chang, Ben J. D. Jou, J. W. Wilson and R. D. Roberts, 2012: Objective prediction of warm season afternoon thunderstorms in northern Taiwan using a fuzzy logic approach, *Wea. Forecasting*, **27**, 1178–1197.

Mueller, C., T. Saxen, R. Roberts, J. Wilson, T. Betancourt, S. Dettling, N. Oien, and H. Yee, 2003: NCAR Auto-Nowcast system. *Wea. Forecasting*, **18**, 545–561.

TABLE 1. The 2x2 contingency table.

		Forecast	
		Yes	No
Observation	Yes	Hit (h)	Miss (m)
	No	False alarm (f)	Correct rejection (c)

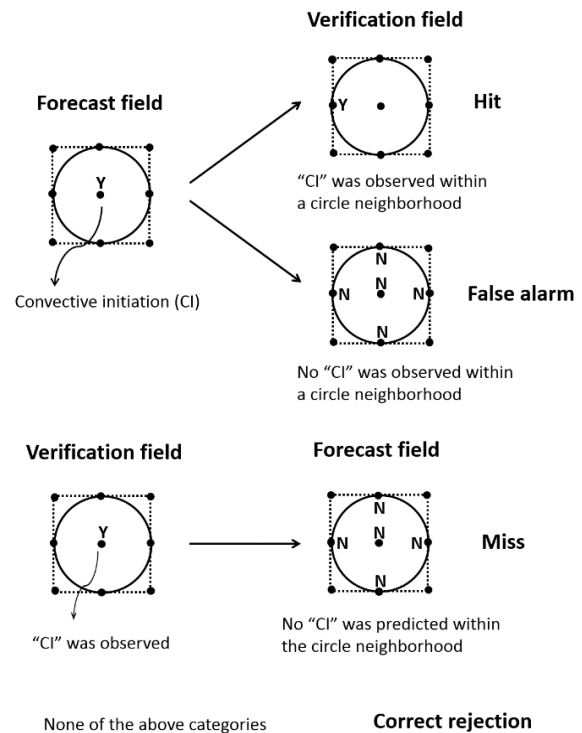


FIG. 1 Spatial relaxation method with $N=1$, which means one grid of storm location displacement is allowed. The circle area is based on this study and the square one is from Lakshmanan et al. (2012).

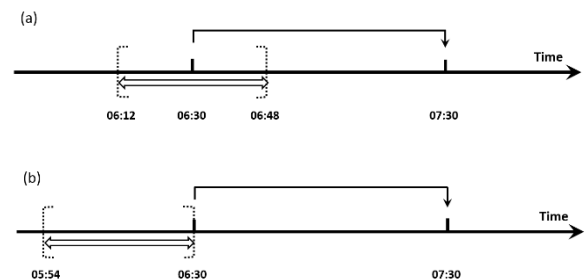


FIG. 2 Schematic diagram of temporal forecasting window. (a) A temporal window of ± 18 min (i.e., 36 min). The nowcast is set at the center of the temporal window (temporal window setting I), and (b) the temporal window size (36 min) is the same as (a), but the nowcast is set at the ending point of the temporal window (temporal window setting II).

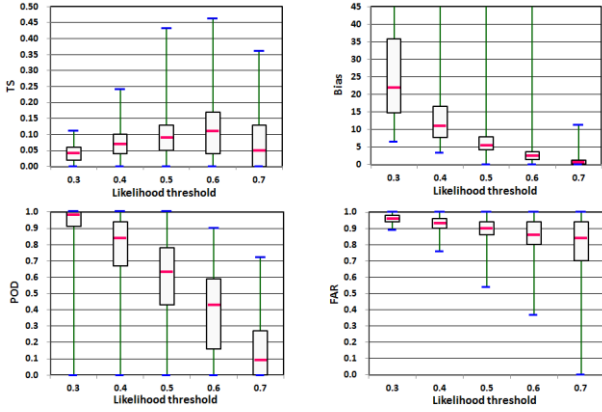


FIG. 3 Boxplots of verification scores for no relaxation at different likelihood thresholds (Lts) from TANC, including TS, BIAS, POD, and FAR.

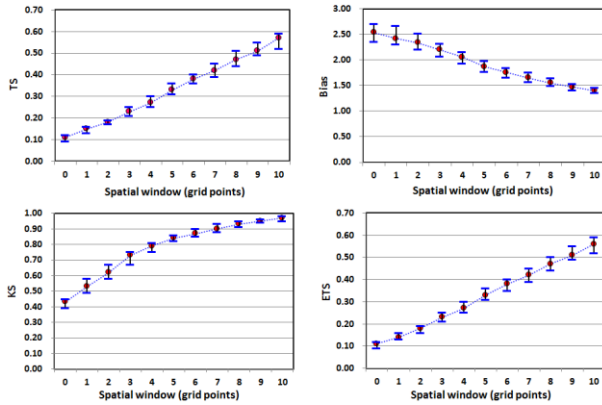


FIG. 4 Score median values and 95% confidence intervals for different spatial windows (grid points) from TANC, including TS, BIAS, KS, and ETS.

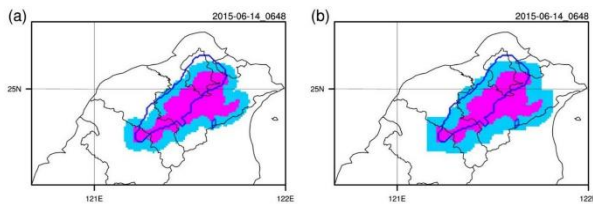


FIG. 5 TANC nowcast product design based on sensitivity tests of scores to different spatial windows using the spatial relaxation of (a) this study and (b) Lakshmanan et al. (2012). The pink shades show the most likely regions for convection initiation (CI) (i.e.,

the areas with likelihood ≥ 0.6). The blue shaded regions show the less likely but still possible areas of CI. The dark blue contours of observed CI are also overlaid for verification. The 1-h TANC nowcast for northern Taiwan was issued at 0648 UTC 14 Jun 2015.

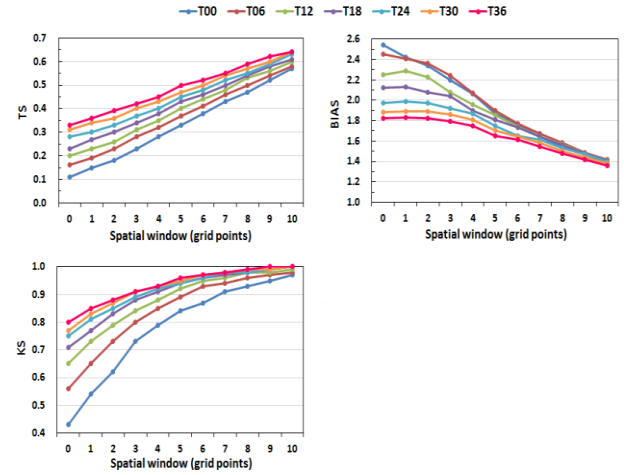


FIG. 6 Score median values for different combinations of spatial and temporal windows (different colored curves) from the TANC, including TS, BIAS, and KS. T00 denotes the temporal point-to-point verification, and T06, T12, ..., T36 represent temporal windows of 6, 12, ..., 36 mins (temporal window setting II).

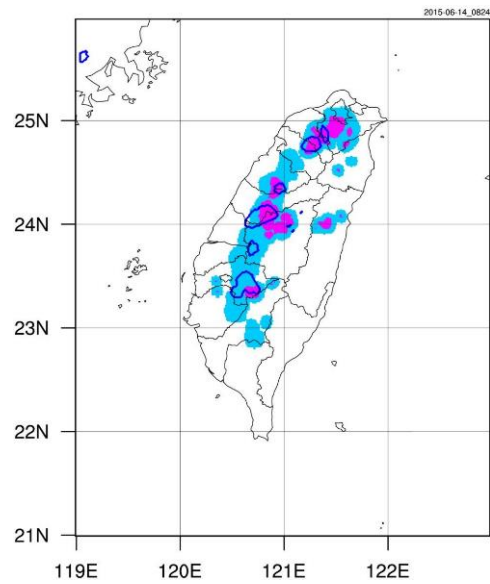


FIG. 7 TANC 1-h nowcast guidance for afternoon convection initiation (ACI) issued at 0824 UTC 14 Jun 2015. The pink shades show the most likely regions for ACI (i.e., the areas with likelihood ≥ 0.6). The blue shaded regions show the tolerable areas of forecast errors (i.e., storm displacement or time shifting). The dark blue contours of observed ACI are also overlaid for verification.